

Anomalous temperature dependence of the single-particle spectrum in the organic conductor TTF-TCNQ

著者	前川 禎通
journal or publication title	Physical review. B
volume	74
number	11
page range	113106-1-113106-4
year	2006
URL	http://hdl.handle.net/10097/40339

doi: 10.1103/PhysRevB.74.113106

Anomalous temperature dependence of the single-particle spectrum in the organic conductor TTF-TCNQ

N. Bulut,^{1,2} H. Matsueda,^{1,3} T. Tohyama,¹ and S. Maekawa^{1,2}

¹*Institute for Materials Research, Tohoku University, Sendai 980-8577, Japan*

²*CREST, Japan Science and Technology Agency (JST), Kawaguchi, Saitama 332-0012, Japan*

³*Department of Physics, Tohoku University, Sendai 980-8578, Japan*

(Received 20 July 2006; published 20 September 2006)

The angle-resolved photoemission spectrum of the organic conductor TTF-TCNQ exhibits an unusual transfer of spectral weight over a wide energy range for temperatures $60 \text{ K} < T < 260 \text{ K}$. In order to investigate the origin of this finding, here we report numerical results on the single-particle spectral weight $A(k, \omega)$ for the one-dimensional (1D) Hubbard model and, in addition, for the 1D extended Hubbard and the 1D Hubbard-Holstein models. Comparisons with the photoemission data suggest that the 1D Hubbard model is not sufficient for explaining the unusual T dependence, and the long-range part of the Coulomb repulsion also needs to be included.

DOI: [10.1103/PhysRevB.74.113106](https://doi.org/10.1103/PhysRevB.74.113106)

PACS number(s): 71.20.Rv, 71.10.Fd, 72.15.Nj, 79.60.Fr

The low-dimensional interacting systems receive attention because of their unusual electronic properties.¹ In this respect, the high-resolution angle-resolved photoemission spectroscopy (ARPES) measurements on the quasi-one-dimensional organic conductor tetrathiofulvalene-tetracyanoquinodimethan (TTF-TCNQ) have provided evidence for non-Fermi-liquid behavior in this compound.²⁻⁵ In particular, the ARPES experiments have found that the single-particle spectral weight at the Fermi wave vector k_F is transferred over an energy range of $\approx 1.3 \text{ eV}$ of the Fermi level in the TCNQ-derived band, as the temperature T decreases from 260 to 60 K.^{3,4} In a Fermi liquid the spectral-weight transfer would have occurred within $\sim k_B T$ of the Fermi level. Here, we investigate the origin of this unusual ARPES data and its meaning for the electronic structure of TTF-TCNQ by using the dynamical density matrix renormalization group (DDMRG), quantum Monte Carlo (QMC), and the exact diagonalization methods.

There are various possibilities as to what might be the origin of the anomalous T dependence of the single-particle spectral weight at the Fermi level, $A(k_F, \omega)$, in TTF-TCNQ:

(i) It has been suggested that the T dependence of the ARPES data can be explained within the one-dimensional (1D) Hubbard model.^{3,4} In this case, the anomalous T dependence of $A(k_F, \omega)$ over the conduction bandwidth has been attributed to the strong-correlation effects. Indeed, by using the Bethe-Ansatz solution, the photoemission spectrum has been fitted excellently to the dispersion of the spinon and holon bands of the 1D Hubbard model with the parameters $t=0.4 \text{ eV}$ for the hopping matrix element and $U=2 \text{ eV}$ for the Coulomb repulsion.

(ii) An alternative point of view is that an extended Hubbard model with long-range Coulomb repulsion is necessary, particularly because the screening of the long-range Coulomb repulsion is expected to be weaker for the surface layer of TTF-TCNQ.

(iii) Another possibility is that the electron-phonon interaction, in addition to the strong Coulomb repulsion, plays a role in producing the unusual T dependence. In this paper, our goal is to differentiate among these possibilities. For this

purpose, we present DDMRG and finite-temperature QMC results on $A(k_F, \omega)$ of the 1D Hubbard model. In addition, we present exact-diagonalization results for the 1D extended Hubbard model which includes a near-neighbor repulsion V and DDMRG results for the 1D Hubbard-Holstein model.

In the following, we show that, above a characteristic temperature determined by the effective magnetic exchange J_{eff} , spectral-weight transfer takes place over a wide energy range in the 1D Hubbard model. This is similar to the T dependence observed in the ARPES experiments. However, below this temperature, the weight transfer is negligible. We find that the Hubbard parameters $t=0.4$ and $U=2 \text{ eV}$ give too large a value for J_{eff} , and with these parameters it is not possible to explain the ARPES T dependence. On the other hand, the $T=0$ exact-diagonalization results on the 1D extended Hubbard model show that the nearest-neighbor Coulomb repulsion increases the bandwidth of the spinon and the holon excitations. This can lead to a smaller value for t for fitting the ARPES dispersions, and a reduced value for J_{eff} , hence, giving better agreement with the ARPES data. In addition, the DDMRG results on the Hubbard-Holstein model show that, at $T=0$, the electron-phonon interaction influences $A(k_F, \omega)$ only at $|\omega| \ll 1.3 \text{ eV}$ for physical values of the phonon frequency ω_0 . However, it remains to be seen how the electron-phonon interaction influences $A(k, \omega)$ at finite T . The main finding of this paper is that the 1D Hubbard model is not sufficient for explaining simultaneously the T dependence and the dispersion of the photoemission spectrum of TTF-TCNQ. We suggest that it is necessary to include at least the long-range part of the Coulomb repulsion.

The Hubbard Hamiltonian H_0 is defined by

$$H_0 = -t \sum_{i,\sigma} (c_{i,\sigma}^\dagger c_{i+1,\sigma} + \text{H.c.}) + U \sum_i n_{i,\uparrow} n_{i,\downarrow}, \quad (1)$$

where $c_{i,\sigma}$ ($c_{i,\sigma}^\dagger$) annihilates (creates) an electron with spin σ at lattice site i , $n_i = n_{i,\uparrow} + n_{i,\downarrow}$, $n_{i,\sigma} = c_{i,\sigma}^\dagger c_{i,\sigma}$, t is the hopping integral, and U is the on-site Coulomb repulsion. We will consider the case of electron-filling $\langle n \rangle = 0.60$, since the filling of the TCNQ band is 0.59. We note that $A(k, \omega)$ of the

1D Hubbard model was studied with the QMC (Refs. 6–9) and the DDMRG (Refs. 8 and 10) as well as with the Bethe ansatz.¹¹

Within the DDMRG method, the single-particle spectral weight is obtained at $T=0$ from

$$A(k, \omega) = -\frac{1}{\pi} \text{Im} \left\langle 0 \left| c_{k,\uparrow}^\dagger \frac{1}{E_0 - \omega - H + i\gamma} c_{k,\uparrow} \right| 0 \right\rangle, \quad (2)$$

where $c_{k,\uparrow}$ annihilates an electron with wave vector k and spin \uparrow , $|0\rangle$ and E_0 are the ground state and the eigenenergy, respectively, and γ is a small positive number. The DDMRG results were obtained with the open boundary conditions. At finite temperatures, we obtain $A(k, \omega)$ by using the determinantal QMC technique.¹² This method yields the single-particle Green's function along the Matsubara time axis, from which $A(k, \omega)$ is obtained by the maximum-entropy analytic continuation.¹³ We have checked the convergence of the maximum-entropy results as the statistics of the QMC data improved. In the following, $A(k, \omega)$ will be plotted in units of t^{-1} . In order to determine the characteristic temperature of the magnetic correlations, we present QMC data on the uniform magnetic susceptibility $\chi(q \rightarrow 0)$ where

$$\chi(q) = \int_0^\beta d\tau \sum_\ell e^{-iq\ell} \langle m_{i+\ell}^z(\tau) m_i^z(0) \rangle \quad (3)$$

with $m_i^z = n_{i,\uparrow} - n_{i,\downarrow}$.

We also present exact-diagonalization results on $A(k, \omega)$ for the 1D extended Hubbard model,

$$H_{ext} = H_0 + V \sum_i n_i n_{i+1}, \quad (4)$$

where V is the nearest-neighbor Coulomb repulsion. The $A(k, \omega)$ of the 1D extended Hubbard model was previously studied with the exact diagonalization technique.¹⁴ In addition, we present DDMRG results on $A(k_F, \omega)$ of the Hubbard-Holstein model defined by

$$H_{HH} = H_0 + \omega_0 \sum_i b_i^\dagger b_i + g \sum_i (b_i^\dagger + b_i) n_i, \quad (5)$$

where b_i^\dagger (b_i) is the creation (annihilation) operator for a dispersionless phonon at site i , ω_0 is the phonon frequency, and g is the electron-phonon coupling constant.

We first discuss DDMRG and QMC results on the 1D Hubbard model. Figures 1(a) and 1(b) show the T dependence of $A(k_F, \omega)$ for $U=5t$ and $8t$. The DDMRG results were obtained for a 60-site chain with 36 electrons, while the QMC results are for a 32-site ring with $\langle n \rangle = 0.60$. Here, the QMC data are shown at selected temperatures because of the numerical cost of these calculations. In the DDMRG calculations we have used a finite energy broadening $\gamma = 0.05t$. For $U=5t$, we observe that the spectral-weight transfer occurs over an energy range $\approx 2t$ of the Fermi level, as T decreases from $0.5t$ down to $0.125t$. However, the weight transfer is negligible between $T=0.125t$ and $T=0$. For $t \approx 400$ meV,^{3,4} $T=0.125t$ corresponds to ≈ 600 K. Hence, in this case, the amount of spectral-weight transfer between $T=600$ K and $T=0$ K is negligible, which disagrees with the ARPES re-

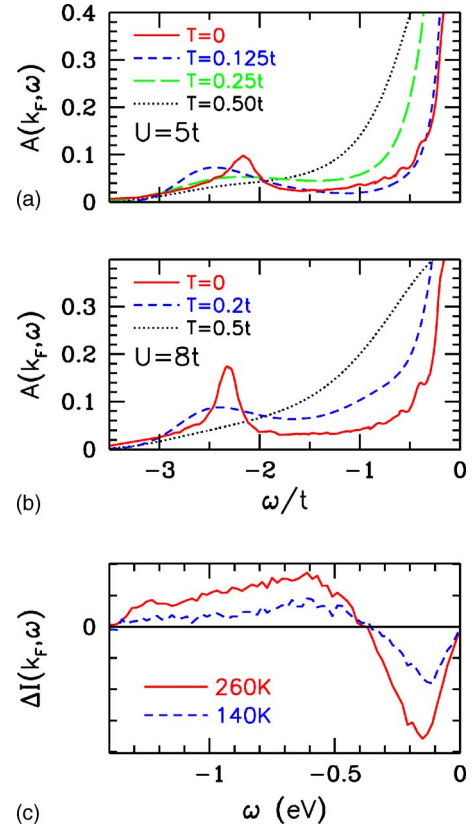


FIG. 1. (Color online) Temperature dependence of the single-particle spectral weight at the Fermi wave vector, $A(k_F, \omega)$, for the 1D Hubbard model with (a) $U=5t$ and (b) $U=8t$. In (c), the change in the ARPES intensity with respect to $T=60$ K, $\Delta I(k_F, \omega)$, is plotted (in arbitrary units) for TTF-TCNQ (reproduced from Refs. 3 and 4 with permission).

sults. In order to study the dependence on U/t , in Fig. 1(b) we show results for $U=8t$. Comparison of Figs. 1(a) and 1(b) shows that the transfer of weight at low T is enhanced for $U=8t$ with respect to $U=5t$. In Fig. 1(c) we show the change in the ARPES intensity at k_F , $\Delta I(k_F, \omega)$, for TTF-TCNQ.^{3,4} These results represent the photoemission intensity arising mainly from the TCNQ-derived band. Here, the solid curve represents the difference in $I(k_F, \omega)$ between 260 and 60 K. The transfer of intensity is also observable as T is lowered from 140 to 60 K (dashed curve). It is considered that, at low energies $|\omega| \lesssim 0.4$ eV, the interchain hopping becomes important.^{3,4} Hence, here we will discuss the energy range -1.3 eV $\leq \omega \leq -0.4$ eV. In Figs. 1(a)–1(c), we observe important differences between the ARPES data and the numerical results. With $U=5t$, it is not possible to explain the low temperature scale of the weight transfer. In addition, we observe that it is not possible to explain the energy range. In the ARPES data, the intensity at -1.3 eV $\leq \omega \leq -0.4$ eV decreases with decreasing T . In the 1D Hubbard model and for $t=0.4$ eV, the decrease of the spectral weight occurs for -0.8 eV $\leq \omega \leq 0$, while the holon peak develops at $\omega \approx -0.85$ eV. Hence, it is not possible to explain the T and ω dependence of the ARPES data using the 1D Hubbard model.

In order to determine the effective magnetic exchange for

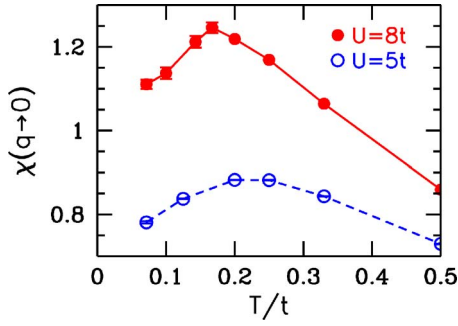


FIG. 2. (Color online) Temperature dependence of the uniform magnetic susceptibility $\chi(q \rightarrow 0)$, plotted in units of t^{-1} , for the 1D Hubbard model. We use these data to determine the effective magnetic exchange.

the 1D Hubbard model, in Fig. 2 we show the T dependence of the uniform magnetic susceptibility $\chi(q \rightarrow 0)$. We obtain a value for J_{eff} by making comparisons with the 1D Heisenberg model. In the 1D Heisenberg model, as T is lowered, $\chi(q \rightarrow 0)$ starts to decrease with the development of the $2k_F$ magnetic correlations, and the maximum of $\chi(q \rightarrow 0)$ occurs at $T_m \approx 0.64J_{eff}$.¹⁵ Obtaining T_m from Fig. 2, we find $J_{eff} \approx 0.35t$ and $\approx 0.26t$ for $U=5t$ and $8t$, respectively. Hence, we have $J_{eff} \approx 1600$ K for $t=0.4$ eV and $U=2$ eV. The results displayed in Fig. 1(a) for $U=5t$ show that the transfer of weight over the wide energy range occurs for $T \geq J_{eff}/3$, implying that this process depends on the development of the short-range magnetic correlations. Apparently, the long-range magnetic correlations are not playing a role in this case. At this point, we also note that $\chi(q \rightarrow 0)$ of bulk TTF-TCNQ is strongly suppressed by the fluctuations of the charge-density-wave (CDW) gap as T decreases from the room temperature down to the CDW transition temperature $T_{CDW}=53$ K.^{16,17}

The density-functional-theory calculations deduce that the hopping parameter $t=0.175$ eV for bulk TTF-TCNQ, while the analysis of the ARPES data yields the Hubbard parameters $t=0.4$ eV and $U=5t$.⁴ This enhancement of t for the surface layer has been attributed to a possible tilting of the TCNQ and TTF molecules at the surface. In this paper, we have seen that the parameters $t=0.4$ eV and $U=2$ eV give $J_{eff} \approx 1600$ K, which is too high to explain the T dependence of $A(k, \omega)$. At this point, we suggest that the long-range part of the Coulomb repulsion might play an important role. For demonstration, we present exact-diagonalization results on $A(k, \omega)$ for the 1D extended Hubbard model with $U=2$ eV. Figure 3 compares $A(k, \omega)$ obtained for $t=0.25$ eV and $V=0.5$ eV with that for $t=0.4$ eV and $V=0$ at wave vectors $k=0$ and $k=\pi/4$. For the 16-site lattice, $k=\pi/4$ is the closest wave vector to k_F . We observe that, at $k=0$ and for $t=0.4$ eV and $V=0$, the holon and spinon branches are located at ≈ -0.68 eV and ≈ -0.27 eV, respectively. For parameters $t=0.25$ eV and $V=0.5$ eV, these structures are located at similar energies. Hence, it is possible to reproduce the locations of the spinon and holon branches by using a reduced value for t within the 1D extended Hubbard model. This behavior is also observed at $k=\pi/4$. Figure 3 also shows that V induces incoherent spectral weight at higher $|\omega|$. For the

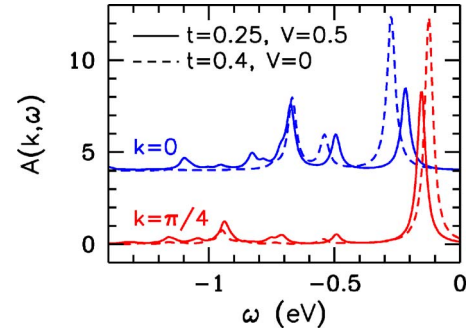


FIG. 3. (Color online) Exact-diagonalization results on the single-particle spectral weight $A(k, \omega)$ at $k=0$ and $k=\pi/4$ for the 1D extended Hubbard model which has onsite and nearest-neighbor Coulomb repulsions U and V , respectively. These calculations were performed for $U=2$ eV on a 16-site ring with 10 electrons corresponding to $\langle n \rangle = 0.625$. Here, spectra obtained for $t=0.25$ eV and $V=0.5$ eV are compared with that for $t=0.4$ eV and $V=0$.

1D extended Hubbard model, we expect $J_{eff} \propto 4t^2/(U-V)$. These results suggest that taking into account the long-range part of the Coulomb repulsion in fitting the ARPES dispersion can lead to a reduced t and, hence, might reduce J_{eff} and the characteristic temperature for the single-particle weight transfer. However, it is necessary to calculate $A(k, \omega)$ for the 1D extended Hubbard model at finite T .

In order to study the effects of the phonons within the presence of the Coulomb interaction, we next present DDMRG results on $A(k_F, \omega)$ for the Hubbard-Holstein model. In TTF-TCNQ, inelastic neutron scattering experiments¹⁸ have revealed longitudinal acoustic and optical phonon modes. The optical branch is weakly dispersive and has a frequency of about 10 meV. Here, we present results for $U=5t$ and an Einstein phonon mode with $\omega_0=0.2t$ and $g=0.2t$. In Fig. 4, we show $A(k_F \approx 6\pi/21, \omega)$ for these parameters on a 20-site chain with 12 electrons. For comparison, we also show results for $g=0$. For the 20-site chain, the finite-size gap Δ_{FS} near k_F is $\approx 0.3t$, and in this figure we have shifted the spectrum by $\Delta_{FS}/2$ so that the main peak in $A(k_F, \omega)$ occurs at $\omega=0$. Because of the finite broadening γ

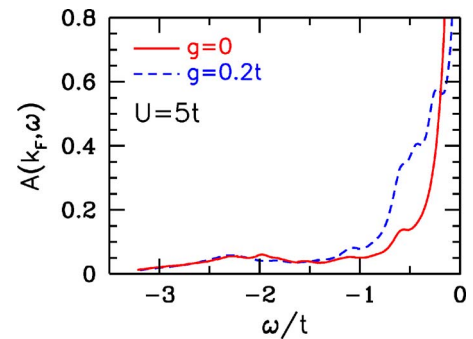


FIG. 4. (Color online) DDMRG results on $A(k_F, \omega)$ of the Hubbard-Holstein model for $\omega_0=0.2t$ and electron-phonon couplings $g=0$ and $g=0.2t$. These results were obtained for $U=5t$ and broadening $\gamma=0.1t$ on a 20-site chain with 12 electrons, for which $k_F \approx 6\pi/21$. This figure shows that, at $T=0$, the electron-phonon interaction with $\omega_0=0.2t$ influences $A(k_F, \omega)$ for $|\omega| \lesssim 1.2t$.

$=0.1t$, we do not observe the opening of the CDW gap. However, we see that the spectral weight at $\omega \approx 0$ is transferred to $-1.2t \lesssim \omega \lesssim -0.2t$. We have performed similar calculations using $\omega_0 = 0.5t$, where multiphonon peaks are induced at energies $\approx -\omega_0, -2\omega_0, -3\omega_0$, etc., with respect to the location of the main peak. For physical values of $\omega_0 \approx 10$ meV, we expect the changes in $A(k_F, \omega)$ at $T=0$ to occur at $|\omega| \ll 1.3$ eV. These results suggest that the electron-phonon coupling is not particularly important for investigating the spectral weight located at -1.3 eV $\lesssim \omega \lesssim -0.4$ eV. However, it is still necessary to study $A(k, \omega)$ of the 1D Hubbard-Holstein model at finite T , since the electron-phonon interaction can influence the T dependence of the magnetic correlations^{16,17} and, hence, the T dependence of $A(k, \omega)$.

In summary, we have studied $A(k, \omega)$ of the 1D Hubbard model in order to investigate the unusual T dependence of the photoemission intensity of TTF-TCNQ. We have also presented $T=0$ results for the 1D extended Hubbard and the 1D Hubbard-Holstein models. We find that in the 1D Hubbard model the transfer of the single-particle spectral weight takes place over a wide energy range above a characteristic temperature, which is too high to explain the ARPES data. We have shown that the long-range part of the Coulomb repulsion can lead to a reduced value for J_{eff} and, hence, to a

better agreement with the ARPES data. Our results on the Hubbard-Holstein model show that, at $T=0$, the electron-phonon interaction does not influence $A(k_F, \omega)$ over the wide energy range observed by the ARPES. In conclusion, these calculations give theoretical support to the notion that the anomalous T dependence of the photoemission spectrum of TTF-TCNQ is due to the strong-correlation effects as suggested by Claessen *et al.*³ However, we also emphasize that the 1D Hubbard model is not sufficient for explaining the unusual T dependence, and at least the long-range part of the Coulomb repulsion needs to be included.

We thank R. Claessen and F. Assaad for useful discussions, and R. Claessen and M. Sing for permission to reproduce their ARPES data. We also thank A. Abendschein and F. Assaad for sending us a copy of their paper (Ref. 9) during the final stage of this project. This work was supported by the NAREGI Nanoscience Project and a Grant-in Aid for Scientific Research from the Ministry of Education, Culture, Sports, Science and Technology of Japan, and NEDO. One of us (N.B.) gratefully acknowledges support from the Japan Society for the Promotion of Science and the Turkish Academy of Sciences (Grant No. EA-TUBA-GEBIP/2001-1-1).

¹J. Voit, Rep. Prog. Phys. **57**, 977 (1994).

²F. Zwick, D. Jérôme, G. Margaritondo, M. Onellion, J. Voit, and M. Grioni, Phys. Rev. Lett. **81**, 2974 (1998).

³R. Claessen, M. Sing, U. Schwingenschlögl, P. Blaha, M. Dressel, and C. S. Jacobsen, Phys. Rev. Lett. **88**, 096402 (2002).

⁴M. Sing, U. Schwingenschlögl, R. Claessen, P. Blaha, J. M. P. Carmelo, L. M. Martelo, P. D. Sacramento, M. Dressel, and C. S. Jacobsen, Phys. Rev. B **68**, 125111 (2003).

⁵T. Ito, A. Chainani, T. Haruna, K. Kanai, T. Yokoya, S. Shin, and R. Kato, Phys. Rev. Lett. **95**, 246402 (2005).

⁶R. Preuss, A. Muramatsu, W. von der Linden, P. Dieterich, F. F. Assaad, and W. Hanke, Phys. Rev. Lett. **73**, 732 (1994).

⁷M. G. Zacher, E. Arrigoni, W. Hanke, and J. R. Schrieffer, Phys. Rev. B **57**, 6370 (1998).

⁸H. Matsueda, N. Bulut, T. Tohyama, and S. Maekawa, Phys. Rev. B **72**, 075136 (2005).

⁹A. Abendschein and F. Assaad, Phys. Rev. B **73**, 165119 (2006).

¹⁰H. Benthien, F. Gebhard, and E. Jeckelmann, Phys. Rev. Lett. **92**, 256401 (2004).

¹¹K. Penc and M. Serhan, Phys. Rev. B **56**, 6555 (1997).

¹²S. R. White, D. J. Scalapino, R. L. Sugar, E. Y. Loh, J. E. Gubernatis, and R. T. Scalettar, Phys. Rev. B **40**, 506 (1989).

¹³W. von der Linden, Appl. Phys. A **60**, 155 (1995).

¹⁴S. Yunoki, T. Tohyama, and S. Maekawa, Physica B **230-232**, 1050 (1997).

¹⁵J. C. Bonner and M. E. Fisher, Phys. Rev. **135**, A640 (1964).

¹⁶J. C. Scott, A. F. Garito, and A. J. Heeger, Phys. Rev. B **10**, 3131 (1974); Y. Tomkiewicz, B. A. Scott, L. J. Tao, and R. S. Title, Phys. Rev. Lett. **32**, 1363 (1974).

¹⁷J. B. Torrance, Y. Tomkiewicz, and B. D. Silverman, Phys. Rev. B **15**, 4738 (1977).

¹⁸J. P. Pouget, S. M. Shapiro, G. Shirane, A. F. Garito, and A. J. Heeger, Phys. Rev. B **19**, 1792 (1979).